"Beam test results on double-gap resistive plate chambers proposed for CMS experiment"

Abbrescia, M. ; Bruno, Giacomo Luca

Abstract

Resistive Plate Chambers were tested in a muon and pion beam to study the performances at different running conditions. Results on a first chamber built without the linseed oil treatment of the bakelite surfaces are presented together with an evaluation of the local effects due to the spacers. These results are extrapolated to the conditions expected at LHC.

Document type : *Article de périodique (Journal article)*

ELSEVIER Nuclear Instruments and Methods in Physics Research A 414 (1998) 135–148

NUCLEAR INSTRUMENTS & METHODS IN PHYSICS RESEARCH Section A

Beam test results on double-gap resistive plate chambers proposed for CMS experiment

M. Abbrescia[a], G. Bruno[a], A. Colaleo[a], G. Iaselli[a], G. Lamanna[a], F. Loddo[a], M. Maggi[a,*], B. Marangelli[a], S. Natali[a], S. Nuzzo[a], G. Pugliese[a], A. Ranieri[a], F. Romano[a], G. Gianini[b], S.P. Ratti[b], P. Vitulo[b]

[a] *Dipartimento Interateneo di Fisica and Sezione INFN, Bari, Italy*
[b] *Dipartimento di Fisica Nucleare e Teorica and Sezione INFN, Pavia, Italy*

Received 1 August 1997; received in revised form 13 January 1998

Abstract

Resistive Plate Chambers were tested in a muon and pion beam to study the performances at different running conditions. Results on a first chamber built without the linseed oil treatment of the bakelite surfaces are presented together with an evaluation of the local effects due to the spacers. These results are extrapolated to the conditions expected at LHC.

1. Introduction

Resistive Plate Chambers (RPCs) are proposed to build large trigger detectors for future experiments at LHC [1]. The expected high counting rate environment requires the detectors to be operated in the so-called avalanche mode [2–4] (low gas gain) which, however, requires front-end amplification. A substantial reduction of charge produced in the gap improves by more than one order of magnitude the rate capability, and allows also the power consumption to be contained within tolerable limits.

In the framework of R&D for CMS, the performances of double-gap RPCs have been under investigation since a few years [5] with encouraging results. This paper reports on further studies of RPCs with the H2 muon beam and defines the milestones for future R&D in order to meet the CMS requirements.

The RPC has to fulfil five basic requirements: high efficiency, good timing, low cluster size, low power consumption and, in the forward region, good rate capability. The maximum expected neutrons and gamma fluxes in the highest η region where the RPCs are foreseen to be installed ($\eta = 2.1$), corresponds (taking into account the RPC sensitivity to neutrons and gamma) to an effective hit rate not more than 300 Hz/cm^2. A rate capability of about 1 kHz/cm^2 is therefore necessary to allow safe operation.

Although some results about performance with high flux pion beam will be presented in this paper,

* Corresponding author.

0168-9002/98/$19.00
PII: S0168-9002(98)00571-3

more tests are necessary with high and uniform background over the whole chamber. These studies are under way at the CERN Gamma Irradiation Facility (GIF) and will be soon available for further analysis.

Also the time distribution of the arriving signals should have a sigma not exceeding 2–3 ns and, furthermore, the base width should be within 20 ns, to allow operation at LHC. It is therefore crucial to avoid, in the time distribution, tail contaminations which could destroy the assignment of the bunch crossing.

The RPC electrodes are usually treated with linseed oil [6]. In view of LHC experiments, such a treatment could affect the detector behaviour: in fact, due to its organic nature, the oil could deteriorate in a high radiation environment, destroying the performances of the system on long-term basis. In addition, the treatment requires quite a long time, and this could result a limiting factor in the procedure of building a large number of chambers.

It was shown [7] that the main effect of the linseed oil is to reduce noise and dark current, and it was suggested that the same effect could be achieved by smoothing a bakelite surface. Such a treatment was used for a new "oil-less" RPC (as described in Section 2); its performance was tested and compared to that of a standard "oiled" RPC.

The response uniformity of a large chamber is also considered a crucial issue for operation at LHC. Variations of the gas gap width, due to mechanical tolerances, may result in local non uniformity of the chamber parameters such as efficiency, time resolution, etc. It is therefore necessary to study global properties averaged over the whole surface, as well as local properties, by illuminating different portions of the chamber with the beam spot.

The paper is organised as follows: the test beam set-up is described in Section 2. Global properties of the new oil-less and of the standard oiled RPCs are presented in Section 3. In Section 4 the results on the measurement of local properties are shown. In Section 5 the results obtained in the two previous sections are used to evaluate the timing performances at LHC conditions.

2. The test set-up

RPCs were tested in the CMS-H2 beam line at CERN SPS during two different periods in 1996. The muon beam, having a Gaussian profile with $\sigma \sim 2$ cm, was set to an energy of 300 GeV/c with a maximum rate of 250 Hz/cm^2. The pion beam, with Gaussian beam spot and $\sigma \sim 1.5$ cm, was used to get rates up to 2.7 kHz/cm^2. The rates were measured with a set of 2×2 cm^2 scintillator

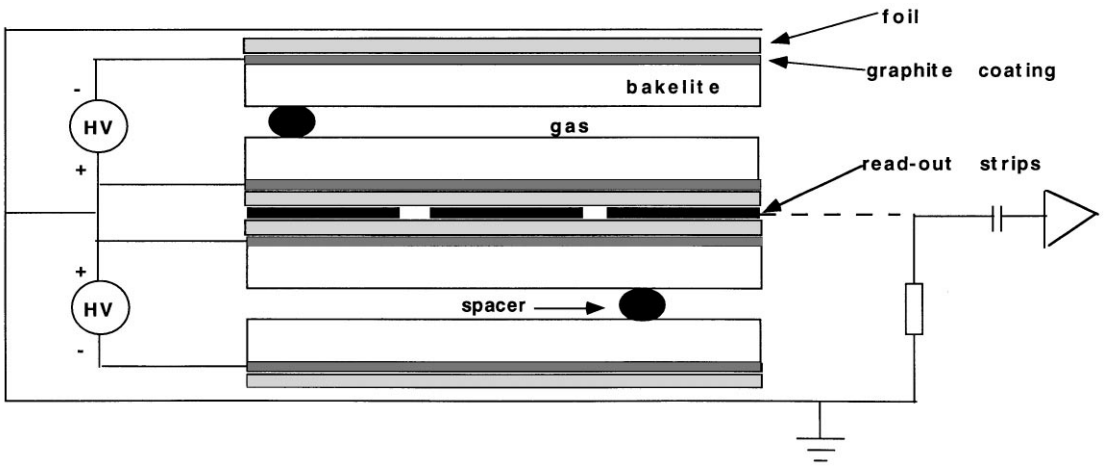

Fig. 1. Cross-sectional view of a double gap RPC.

counters over a region centred on the beam, during the 2.5 s spill.

The trigger system, based on several scintillators, produces a trigger signal with less than 0.5 ns jitter on the $10 \times 10\,cm^2$ or $2 \times 2\,cm^2$ areas of the chamber. In the two separate periods, data were collected under different experimental conditions.

The first period was devoted to the comparison of the global performances of two different CMS-like double gap RPCs. The chambers had $50 \times 50\,cm^2$ area and 2 mm gap width. The read-out strips, located between the two gaps, were 1.3 cm wide with 1.5 cm pitch (Fig. 1). The resistive electrodes were made of bakelite plates. The surfaces of the bakelite plates of one chamber were treated with linseed oil. The other chamber was built with new bakelite plates exhibiting good improvement on the quality of the surface, obtained by using more refined tools in the production procedure.

The chambers were operated with two gas mixtures: the first was based on $C_2H_2F_4$ (90% $C_2H_2F_4$, 10% i-C_4H_{10}); the second was based on Argon (70% Ar, 15% $C_2H_2F_4$, 10% CO_2, 5% i-C_4H_{10}). Although there might be concern about the flammability of the $C_2H_2F_4$ mixture, for the moment we prefer to maintain the i-C_4H_{10} percentage at the level of 10% in order to have backward compatibility with other data taken in previous runs. Variation of a few % of i-C_4H_{10} does not significantly affect the performance, as reported by other groups [8]. A prototype Cathode Strip Chamber, under test in the same beam line, was used as multi-tracks veto.

A second period was devoted to study specifically local properties of the chambers. A $50 \times 50\,cm^2$ double gap RPC, with 2 mm gap width and oiled bakelite plates, operated with the $C_2H_2F_4$-based mixture, was placed between two "beam chambers" able to determine the impact point on the RPC of the incoming particle with a resolution of 0.2–0.3 mm.

In both the running periods the RPCs were equipped with hybrid front-end preamplifiers. The input impedance of the preamplifier is set to match the strip characteristic resistance of 40 Ω; the rise time of the delta impulse response is 1.5 ns. The linear dynamic range is limited to ~ 500 fC and the charge sensitivity, in this range, increases from 1 mV/fC (at $Q = 10$ fC) to 2 mV/fC (at $Q = 500$ fC). This is due to the increasing transconductance of input transistor as the injected charge increases. The noise, when the strip is connected, is determined mainly by the 40 Ω passive termination of the far end strip. The equivalent noise charge is ~ 1.8 fC, corresponding to 1.8 mV-rms output noise. However, in the present experimental conditions the total output noise, including pick-up, was less than 3 mV-rms.

To measure efficiency, timing and cluster size, the amplified signals were discriminated with 30 mV (first set of measurements) and 10 mV (second set of measurements) thresholds, before feeding a common start Time-to-Digital Converter (TDC) with 100 ps sensitivity. The charge was measured by feeding the signals (after amplification with a Lecroy 612AM) to an ADC having 250 fC bin width. The arrival time of an RPC signal was always measured with respect to the trigger signals. The efficiencies were defined as the ratio between the counting rate of the signals above threshold and the trigger rate, within a 200 ns window.

3. Global performances

3.1. Efficiency and rate capability

In Fig. 2, the efficiency of oiled and oil-less chambers is shown versus the applied high voltage for the two gas mixtures, at different rates. In the same figure the streamer probability is also shown. Streamer probabilities were measured in dedicated runs at a very low rate, by counting the number of events with charges larger than 13 pC.

Of course, the chambers show an efficiency depletion with increasing rate, and this is caused by the corresponding decrease of the effective voltage applied to the gap. Moreover, at high rate, the measurements show that the efficiency decreases also as a function of the elapsed time from the start of the spill. This can be seen in Fig. 3: at $1\,kHz/cm^2$ the chamber is still rather stable, while at $2.7\,kHz/cm^2$ the chamber does not reach any stationary condition within the 2.5 s spill. Therefore, efficiencies shown in Fig. 2 at the highest rate may be overestimated.

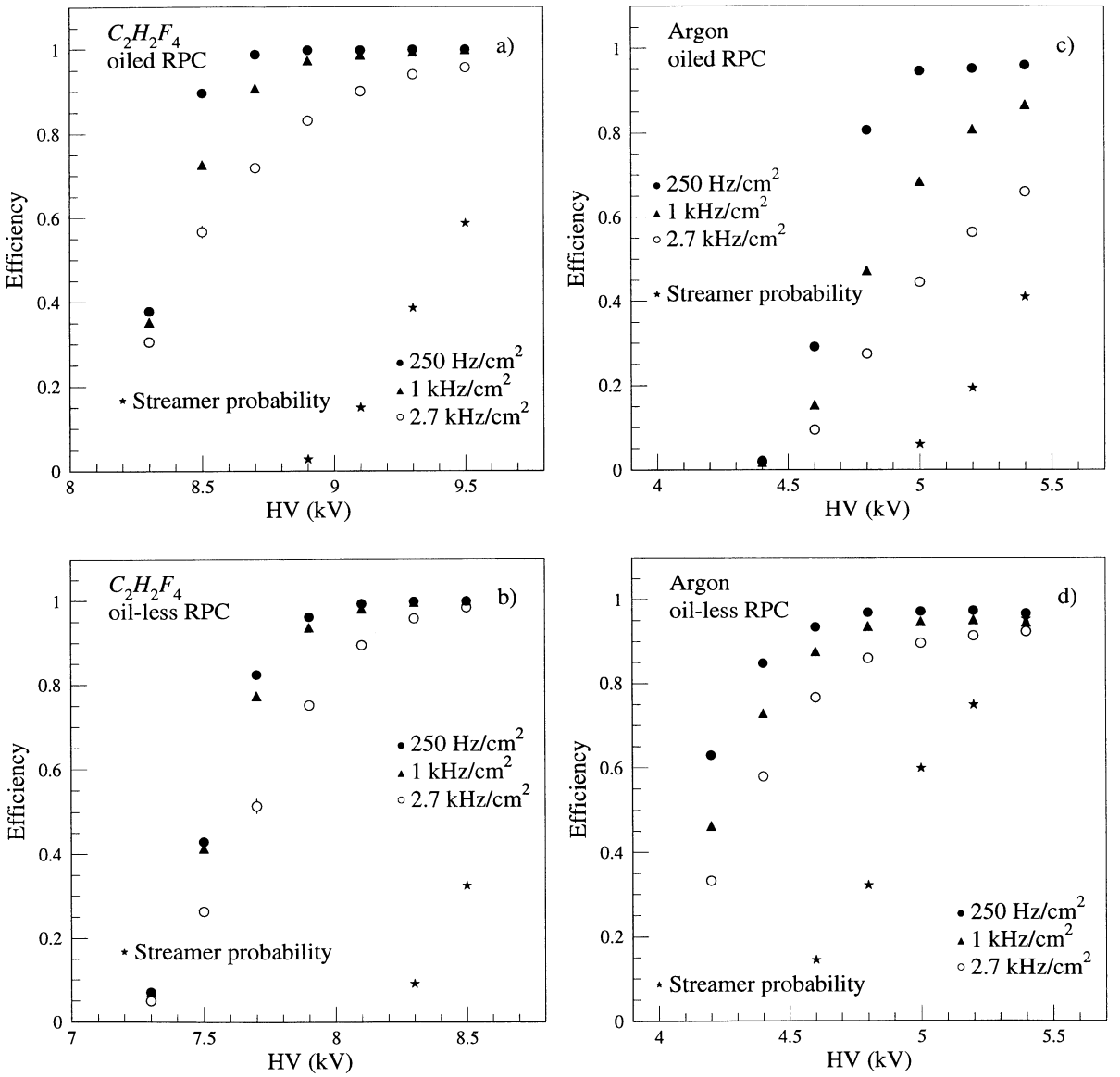

Fig. 2. RPC efficiency plateau curves. (a, b) Results obtained with $C_2H_2F_4$ based mixture; (c, d) results obtained with argon based mixture.

The singular behaviour of efficiency versus time deserves a comment. Fig. 3 can be interpreted as the *efficiency transient response* of the detector: the 'input' is a step increase of rate; the 'response', observed during the spill window, is the efficiency. The high flux of the incoming ionising particles discharge the bakelite plate with a rate initially larger than the rate of the re-charge process given by the external supply, until a dynamical equilibrium is reached. The detailed study of the transient response of the detector needs a more careful analysis and is beyond the scope of this paper.

The gap voltage drop at equilibrium is $\Delta V = RI = \rho d\bar{q}(r)r$, ($\bar{q}(r)$ being the rate-dependent

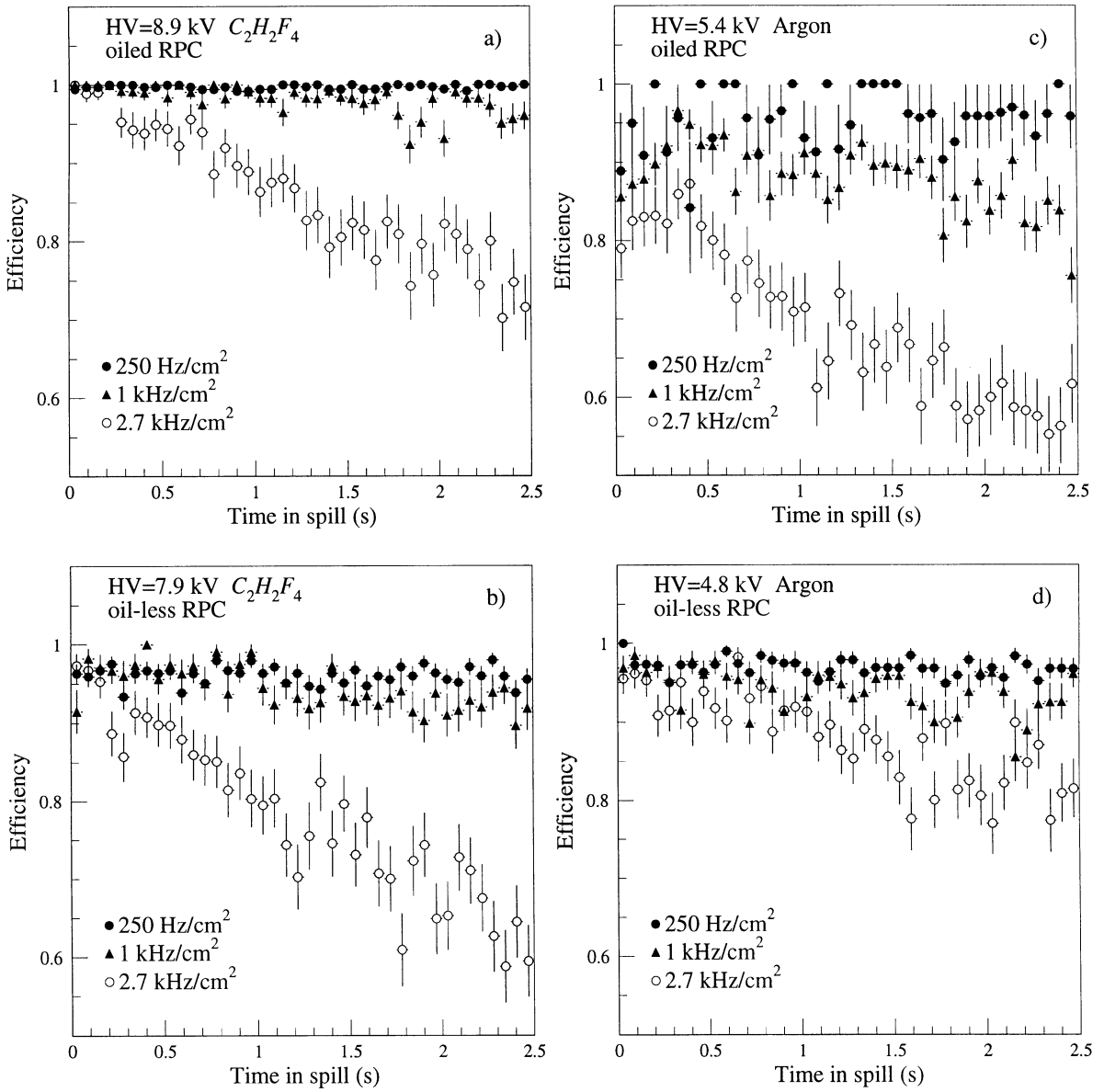

Fig. 3. RPC efficiency versus time elapsed from the start of the spill. (a, b) Results obtained with $C_2H_2F_4$ based mixture; (c, d) results obtained with argon based mixture.

average charge per avalanche, r being the rate per unit area and d being the total bakelite thickness). The effective voltage on the gas gap is lower than the one supplied. Since, in case of streamer free operation, $\bar{q}$ in argon mixture is much less than that in $C_2H_2F_4$ [9], ΔV is smaller in argon than in $C_2H_2F_4$, being the streamer probability is negligible at the effective voltage reached by the chamber. This could explain the different behaviour of the two mixtures, shown in Fig. 3.

The transient response shows that Argon is more robust than $C_2F_2H_4$ against possible rate

fluctuations, expected in LHC environment. However, operation with Argon is affected by higher streamer probability (that however needs to be studied at higher rate), worse time resolution, and requires a lower threshold of the discriminator.

As $\bar{q}$ can be only marginally controlled, the major interest appears to be the influence of bakelite resistivity: the voltage drop decreases by reducing the resistivity, and a better high rate performance should be expected.

3.2. Time resolution

As known [5], the charge signal induced by a single cluster can be expressed as

$$Q(t) = \left(\frac{n_0\ q_e}{\eta d}\right)\exp(t/\tau'),$$

where n_0 is the number of primary electrons, q_e, the electron charge, d, the gap width; $\tau' = 1/\eta v$, the gas time constant; v, the electron drift speed; η, the effective Townsend coefficient.

The time resolution of an RPC is determined by a number of sources, namely physics of the ionisation processes, electronics, technology of the detector (field variations due to gap non uniformity and the presence of the spacers).

The contributions due to the ionization originate from statistical fluctuations of the number and size of primary clusters that give rise to a detectable signal. In addition there are contributions from statistical fluctuations in the avalanche gain, space-charge effects and interaction between avalanches of single clusters [10].

All these fluctuations cause the amplitude, the rise time, and the arrival time of the induced signal to change, so that signals will cross a given threshold at different times. Looking at the average timing error (walk), only the contribution due to the changing amplitude and rise time (slewing) can be corrected by electronic means, like a constant fraction discriminator (CFD). The contribution due to changing arrival time would be unaffected (by "arrival time" we mean the time the signal takes to exceed the noise).

The intrinsic contribution of the electronics to the timing error is twofold. The first is an additional slewing introduced by the leading-edge comparator: the input signal causes an increasingly delayed response as its amplitude approaches the threshold. This effect is well known and is due to the finite gain-bandwidth product of the comparator circuit. It could be corrected by a CFD.

The second intrinsic contribution is due to the amplifier noise, and is given by

$$\sigma_{t1} = \frac{\sigma_n}{(\mathrm{d}V/\mathrm{d}t)},$$

σ_n being the integrated noise at the discriminator input, and $\mathrm{d}V/\mathrm{d}t$ the signal slope at the threshold. As already discussed, the noise in our case is less than 3 mV rms. The average signal slope could be evaluated analytically, knowing the signal shape and using the normalised charge spectrum as weighting function. In our case, we find that $\langle \mathrm{d}V/\mathrm{d}t \rangle \sim 6\,\mathrm{mV/ns}$. Thus, $\langle \sigma_{t1} \rangle$ is less than 0.5 ns. Of course, this error is unaffected by any of the slewing correction technique.

The total time slewing has been simulated using Pspice, and measured using a test pulse having the same rise time as RPC signals. The reader can find in Ref. [11] the results related to the integrated version of our front–end electronics. For the processing chain used here (hybrid amplifier + Lecroy Mod. 620CL discriminators) the total slewing curve has the same behaviour as that shown in Fig. 5.6.5 of Ref. [11]; it is shifted only by + 20 ns, mainly due to the propagation delay of the Lecroy discriminator. This slewing curve represents a delay measured from the signal origin. This means that the arrival time of the signals are possibly different, with respect to the absolute time origin when the particle crosses the detector, and are not accounted for in this measurement.

The timing error due to the slewing can be evaluated by convoluting the total delay and the normalised charge spectrum. This was done using charge spectra taken in many different conditions: the rms error was always $\sigma_{t2} = 0.7$–0.8 ns.

There are contributions due to the detector technology: the spacers between the electrodes cause a distortion of the electric field inside the gap, and this distortion extends to surrounding area. Mechanical tolerances and roughness of bakelite

surface cause uneven gap width, thus still local field distortions. Now, variations of the electric field cause variations of η. Furthermore, the electron drift speed changes as well. Anyway, a change in the gas time constant τ' causes both a change in the average signal arrival time and rise time. This moving arrival time cannot be compensated by a CFD.

Fig. 4 shows the measured time resolution versus the incoming beam particle rate. Resolution becomes worse with increasing rate, indicating that variations of gas time constant, due to the

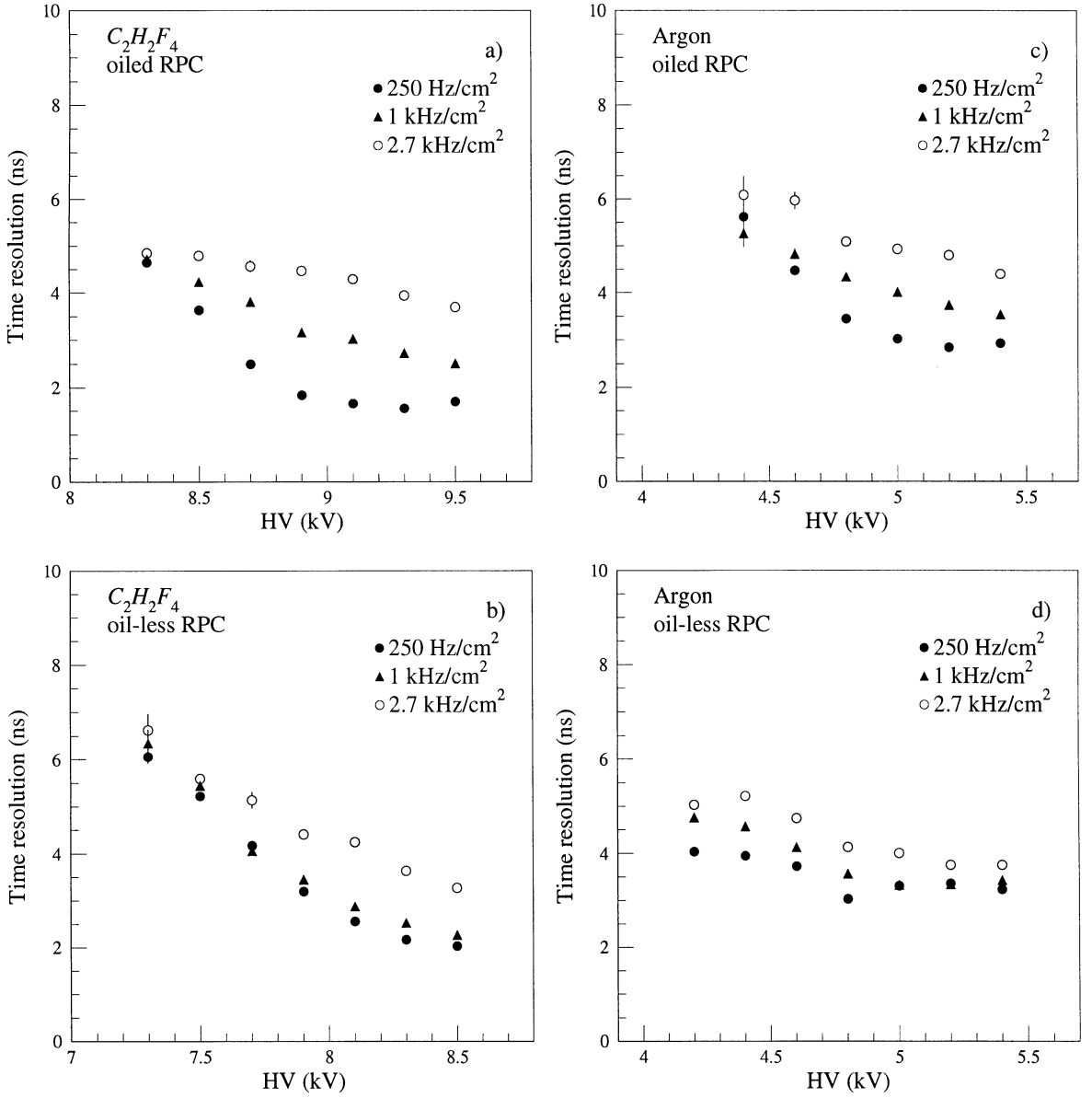

Fig. 4. Time resolution of the chambers. (a, b) Results obtained with $C_2H_2F_4$ based mixture; (c, d) results obtained with argon based mixture.

dynamical behaviour of the chamber, become more and more important at higher rates. Also, time performances obtained with the argon mixture are clearly poorer. This is due to the lower drift velocity and lower primary ionisation density of this gas as compared to the $C_2H_2F_4$ mixture.

Now, looking at the contributions of the noise ($\sigma_{t1} = 0.5$ ns) and of the time slewing ($\sigma_{t2} = 0.7$ ns), and comparing them to the total experimental $\sigma_{tot} \sim 2$ ns, one can conclude that in RPC signal processing the electronics plays only a marginal role. Introducing a CFD in the channel would add negligible benefits.

We can ascribe to the changing mean arrival time of signals the main contribution to timing error. This contribution is partly intrinsic to the physics of ionisation and partly due to the still poor detector technology: efforts to reduce timing error should be concentrated in this direction.

3.3. Cluster size

Measurement of intrinsic cluster size of the detector was affected by the presence of the electrostatic coupling between the electronic channels, in addition to the intrinsic crosstalk between the strips. The coupling caused signals having amplitude approximately 10% of the primary signal and rather delayed with respect to this one.

In order to isolate the intrinsic contribution of the detector, one should take into account that the propagation delay of crosstalk pulses inside the chamber is of the same order as that along the strips. Thus, the cluster size is computed around the fastest fired strip by counting the number of adjacent strips fired within 10 ns. The mean cluster size versus High Voltage is shown in Fig. 5. It grows since an increasing charge is produced in the chamber, causes a large amount of crosstalk. The depletion of cluster size at high rate might be interpreted as due to the decrease of the produced charge, since as already mentioned the effective voltage applied to the gap decreases as the rate increases.

From inspection of Figs. 2–5, we can conclude that the oil-less RPC with improved surfaces shows performances similar to those of traditional oiled one. Moreover the $C_2H_2F_4$ mixture seems suitable for LHC conditions at rates not exceeding 1 kHz/cm^2 with the present bakelite resistivity ($\approx 10^{11}\,\Omega$ cm). At very high rates, little can be said since the spill length prevents us from drawing any firm conclusion.

4. Local effects

In the present detector design, gap width and mechanical stability of each single module are assured by a set of cylindrical spacers, having 8 mm diameter, located, for each gap, in a grid of 10 cm pitch. The spacers of the two gaps are staggered by 5 cm, in the direction orthogonal to the read-out strips.

The local behaviour of a standard RPC was studied in detail to determine any possible spacer effects on the performances. The impact point of the incoming particle is interpolated from the "beam chamber" measurements for each triggering particle.

The muon beam, used for this analysis, was triggered by the 10×10 cm^2 counters. Data samples were collected at two positions of the chamber, 10 cm apart, along the read-out strip. In what follows, only data taken with the oiled chamber is discussed.

When a spacer is hit by an ionising particle, only one gap of the chamber contributes to the signal. The charge collected on the readout strips is therefore reduced, lowering the efficiency. However, the presence of the spacer affects a region exceeding its physical dimension.

Fig. 6 shows the inefficiency of the RPC, operated at 8.7 kV, in cells of dimension 0.8×0.8 cm^2 (well above the space resolution for the entrance point of the particle, estimated to be 0.2–0.3 mm). The highest inefficiency corresponds to the spacers location. It is interesting to note that the area affected by the presence of a spacer is 5 cm^2. It turns out that, although the grid of spacers only covers 1.3% of the total area of the chamber, performance may be degraded on an area as large as 10% of the total. The overall efficiency of the chamber versus High Voltage was then calculated as the mean of the local efficiencies. The results agree with those described in the previous section and shown in

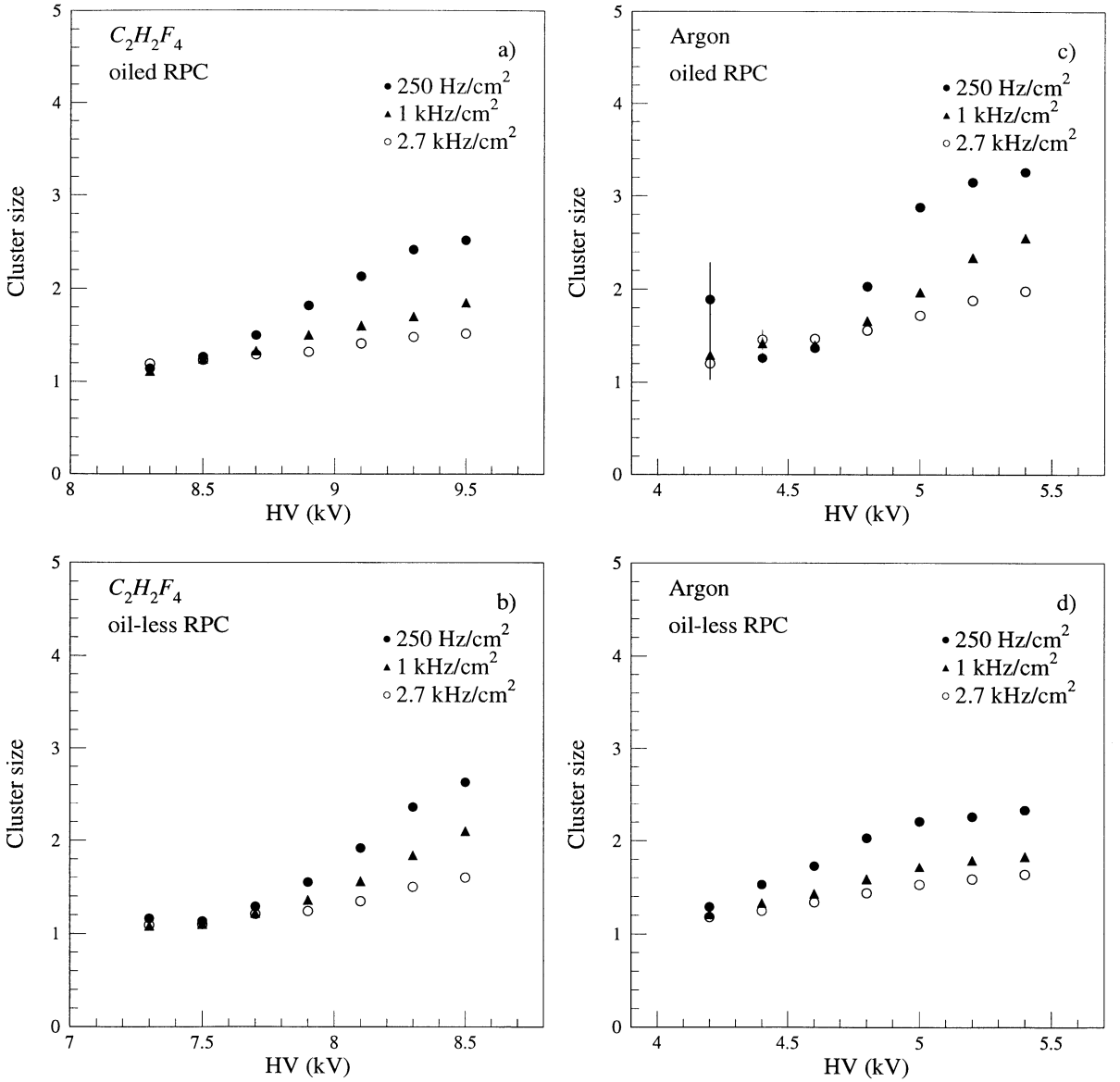

Fig. 5. Mean cluster size. (a, b) Results obtained with $C_2H_2F_4$ based mixture; (c, d) results obtained with argon based mixture.

Fig. 2a, and are then representative of the overall behaviour of the chamber.

Fig. 7 shows the charge distributions at different positions in the chamber. The spectra are given in arbitrary units, since we are interested only in the relative variations. Less charge is involved in the avalanche development, when this occurs in proximity of a spacer, the charge spectrum is essentially that of a single gap. In addition, it can be seen that the average charge is about half that of distant areas, where the spectrum is the convolution of that of two single gaps.

From Fig. 7 one can clearly see the advantage of the double-gap system, which allows an efficiency

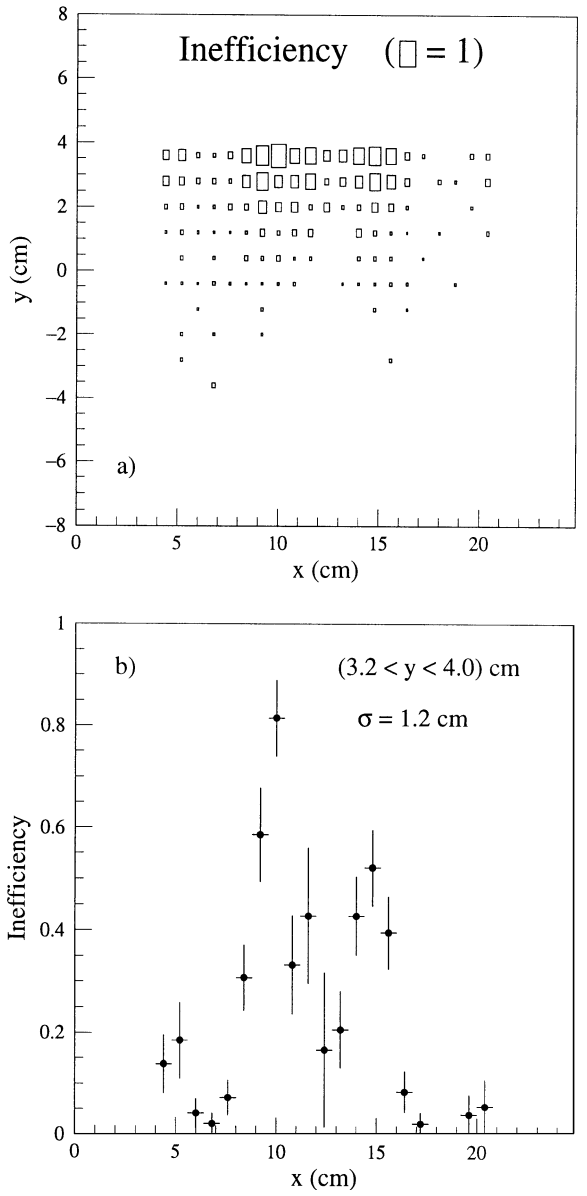

Fig. 6. Oiled RPC, operated with $C_2H_2F_4$ at 8.7 kV; inefficiency as a function of the incoming beam particle position. (a) The box's size is proportional to the inefficiency measured in the 0.8×0.8 cm^2 cell. The x-direction is along the strips, while the y-direction is perpendicular to the strips and the beam. Maximal inefficiency corresponds to the spacer's position. (b) The dots show the inefficiency measured along x for $3.2 < y < 4$ cm. The error bars are statistical errors. The widths of the distributions around the spacers are ~ 1.2 cm.

higher than that of a single-gap detector using the same threshold.

Charge spectrum, in both cases, is well reproduced by the Monte Carlo simulation [12]. Other results on single-gap charge spectrum have been reported in literature in various conditions of operation [8,13]. Spectra obtained in conditions similar to the ones described in this paper, substantially agree with our results. However, any change in experimental conditions, like gas gain and composition, noticeably affect the shape of the spectrum.

Timing properties were also studied locally. Events were selected by requiring the incoming particle to be within the area of a given strip, so that all the events were read out by the same electronic channel. Then, for each strip the data sample was subdivided into 0.8 cm slices along the strip. The following results are obtained with the RPC operated at 8.7 kV.

Fig. 8 shows the mean and the width for the distributions of the signal arrival time along two strips, one with an underlying spacer (full dots) and the other 3 cm apart (open squares). Time distributions of each slice, far from the spacers, turns out to be approximately Gaussian with $\sigma \sim 1.5$ ns.

Many interesting results can be observed in this figure. The first is that the mean values of local distributions are sensibly larger when the slice is near a spacer, where the electric field is reduced. This seems to confirm an increase of the mean arrival time of signals, that is, an increase of the gas time constant. Also, when the slice is just on a spacer, only one gap is active; the available charge becomes one-half and the slewing suddenly increases.

The second observation is that, apart from the spacer region, one should expect a mean arrival time almost independent of the distance of the slice from the amplifier (placed at the right end of Fig. 8). In fact, the propagation delay along the strip is 5.5 ns/m. For the moment we cannot explain surely the noticeable decrease shown in the figure as the slice gets closer to the amplifier. It could be simply ascribed to a gap non-uniformity and to the consequent variation of the gas time constant. However, we plan to study more carefully this phenomenon on a small chamber having a variable gap width.

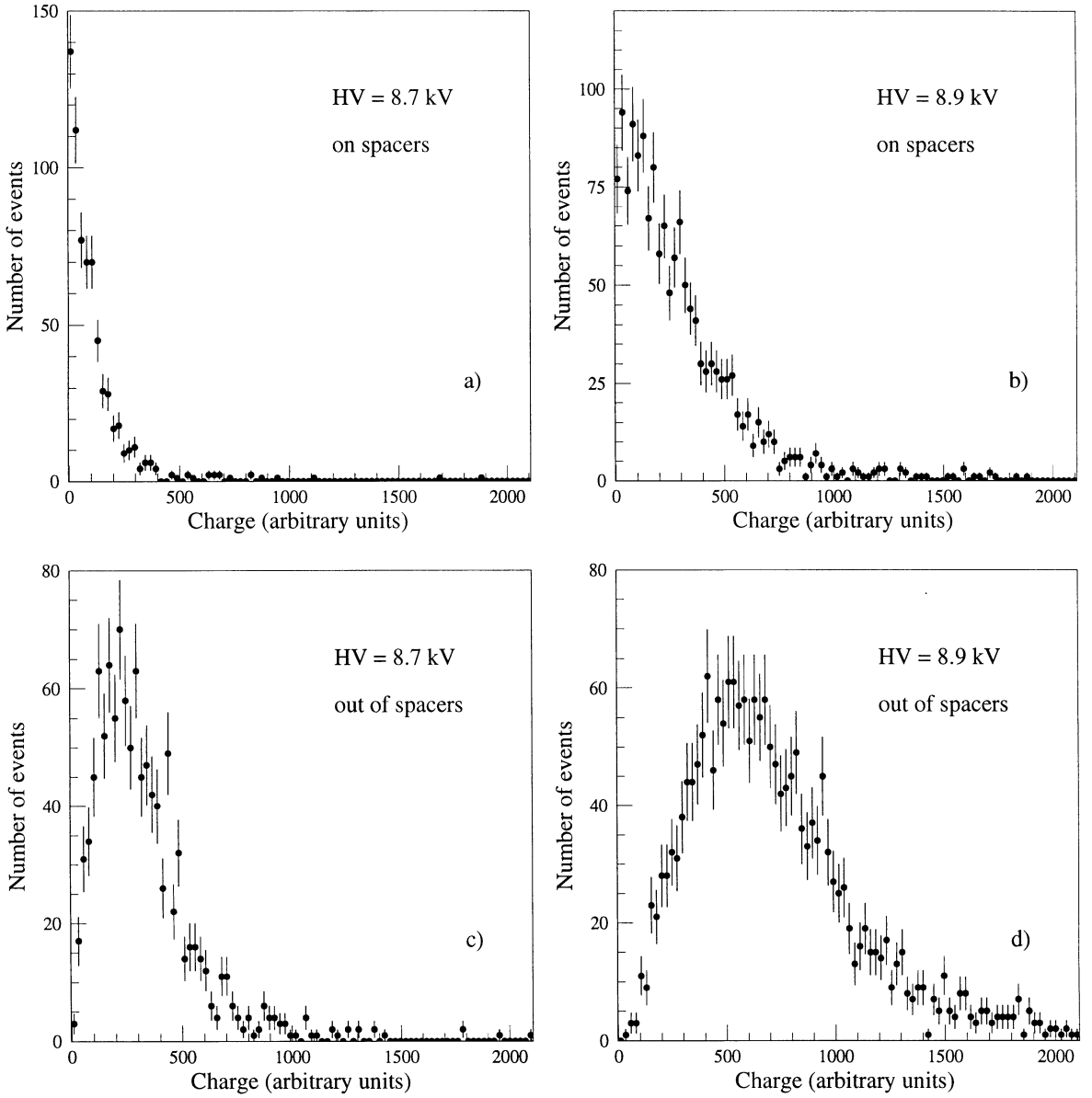

Fig. 7. Charge distributions measured by selecting beam particles crossing; (a, b) strip facing the spacers; (c, d) strips far away from the spacers.

Finally, we observe that the timing behaviour of a single slice is a local detector property, unaffected by the technology. Thus, the $\sigma \sim 1.5$ ns is likely caused by the time slewing ($\sigma_{t1} = 0.7$ ns), by the noise ($\sigma_{t2} = 0.5$ ns), and by the changing mean arrival time only due to the physics of ionisation. This last contribution can be evaluated in turn, obtaining $\sigma_{t3} \sim 1.2$ ns. If we assume that the contribution of the changing arrival time caused by the technology is the same as that of the ionisation, we get a $\sigma_{tot} \sim 1.9$ ns, close to the experimental value of 2 ns for the whole chamber.

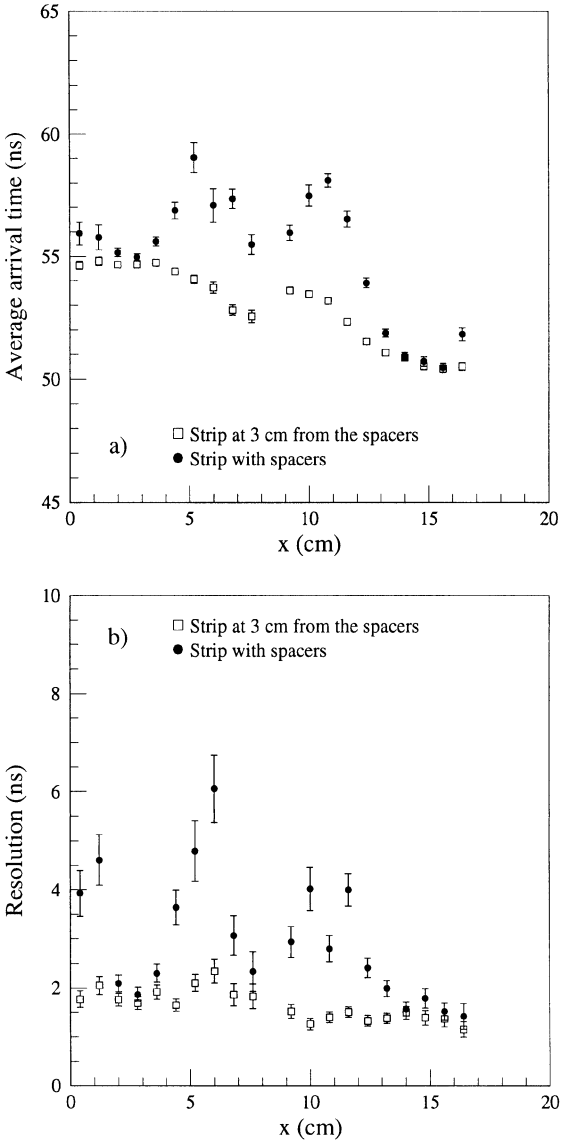

Fig. 8. Local time respone as a function of the x-position. (a) Average time; (b) resolution computed as the root mean square of the distributions. The full dots represent the results obtained for the strip facing the spacer while the open squares are the results for the strips at approx. 3 cm from the spacers. The bars are the statistical errors of the measurements.

The time distribution for the whole chamber is shown in Fig. 9. It has non-Gaussian tails that are attributed to the differences in the mean arrival time of the signals coming from different points,

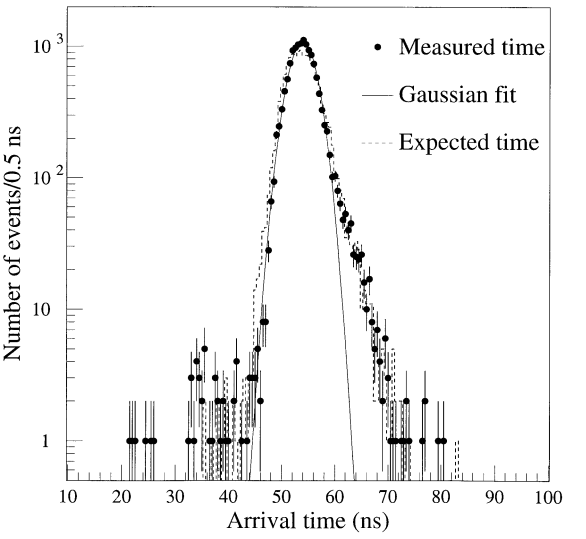

Fig. 9. RPC overall time distribution. The solid histogram is obtained by considering the arrival time of the signals with respect to the trigger signal. The solid curve is the result of the fit to a Gaussian distribution. The dashed histogram represents the result of the calculation described in the text.

spacers are also included. To confirm this hypothesis, a simple study was performed of summing Gaussian distributions with means and widths as measured in each slice, and weights given by the measured local efficiency. The result of the simulation, shown in Fig. 9 as the dashed histogram, and overlaps nicely with the experimental distribution.

5. Evaluation of timing performances at LHC

Good time performances are crucial for triggering with high efficiency at the LHC conditions. In particular, since the beam crossing is foreseen every ≈ 25 ns, the RPCs are expected to give a trigger signal within such a time to identify the bunch crossing.

Poor time resolution may reduce the trigger efficiency. Moreover, the indetermination of the impact point of the particle along the strip introduces an additional fluctuation of the time delay (≈ 5 ns/m) which must be accounted for. This effect increases the measured resolution by an additional term in quadrature of the order of $5\,\text{ns}/\sqrt{12}$.

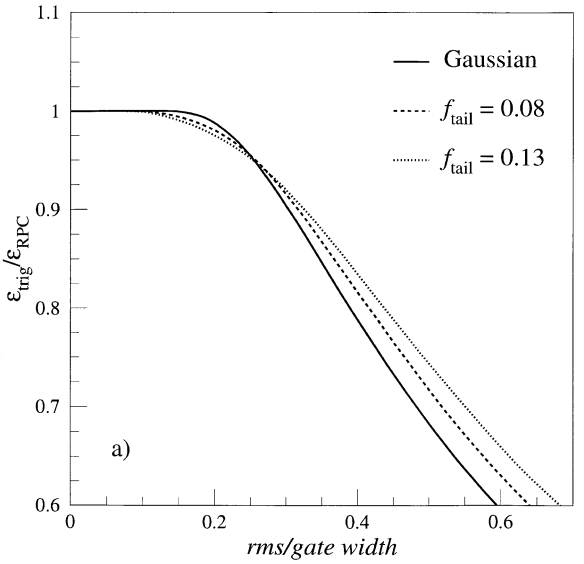

Fig. 10. Ratio between the trigger efficiency ε_{trig} and the RPC intrinsic efficiency ε_{RPC}, as a function of the time resolution normalised to the gate width.

Of course, to obtain high trigger efficiency, the gate window, which enables the read-out, should be centered with the appropriate precision at the average arrival time of the signals. Even in the best case, a signal arrival time distribution with significant tail exceeding the gate window, may results in a loss of the trigger efficiency.

Therefore to evaluate realistic performances, the effects of non-Gaussian tails of the time distribution, expressed as

$$f_{tail} = 1 - \sigma/rms$$

must be considered.

Fig. 10 shows the ratio of the trigger efficiency ε_{trig}, within the gate, to the RPC intrinsic efficiency, at different values of parameter *rms/gate width*. Three typical cases are considered:

1. a pure Gaussian time distribution ($f_{tail} = 0$),
2. the time distribution shown in Fig. 9 ($f_{tail} = 0.13$),
3. a time distribution where fluctuations due to the strip length arise (1.3 m) are included ($f_{tail} = 0.08$).

For example, in the more realistic case (iii), a trigger efficiency loss of 3% is expected, for a 20 ns gate, if the *rms* of the time distribution is 4.4 ns.

The results of the test beam runs have shown that the RPCs operated in $C_2H_2F_4$ at full efficiency, once the length of the strip is accounted for, have a time resolution well within 4 ns.

As mentioned at the beginning of this section, the absolute time also at which the read-out gate window is opened is important. A *time plateau* can be defined as the time region in which the gate may be moved without significantly affecting the trigger efficiency. We find that, again in the case of a 20 ns gate, a time plateau of 4 ns is available, if a 3% loss of trigger efficiency is allowed.

6. Conclusions

Test beam results obtained at the H2-CMS beam line show that Resistive Plate Chambers can operate as trigger devices for LHC up to 1 kHz/cm^2. The first chamber without linseed oil treatment on the bakelite surfaces was successfully operated with performances that are comparable to those of a oiled detector. The effects of local non-uniformity were evaluated. The main impact is a slight degradation of the time resolution, however well within the limit of 4 ns, at which the chamber would loose 3% efficiency if operated with a 20 ns read-out gate.

Acknowledgements

We would like to acknowledge the helpful support of G. Bencze and F. Szoncso at the CMS-H2 beam line. We wish to thank P. Giacomelli and D.A. Chrisman for their help in analysing the CSC data. We are also grateful to the technical staff of the Bari and Pavia groups for their excellent work.

References

[1] CMS Collaboration, Technical Proposal, CERN/LHCC 94-38, 15 December 1994.
[2] R. Cardarelli et al., Nucl. Instr. and Meth. A 333 (1993) 399.

[3] I. Crotty et al., Nucl. Instr. and Meth. A 337 (1994) 370.
[4] C. Bacci et al., Nucl. Instr. and Meth. A 352 (1995) 552.
[5] M. Abbrescia et al., Nucl. Instr. and Meth., A 398 (1997) 173.
[6] R. Santonico, R. Cardarelli, Nucl. Instr. and Meth. 187 (1981) 377.
[7] M. Abbrescia et al., Nucl. Instr. and Meth. A 394 (1997) 13.
[8] ATLAS Muon Collaboration, ATLAS Muon Technical Design Report, CERN/LHCC 97-22, 5 June 1997.
[9] M. Abbrescia et al., Nucl. Instr. and Meth. A 392 (1997) 155.
[10] E. Cerron Zeballos et al., Nucl. Instr. and Meth. A 381 (1996) 569.
[11] CMS Collaboration, CMS Muon Technical Design Report, CERN/LHCC 97-32, 15 December 1997.
[12] M. Abbrescia et al., Nucl. Instr. and Meth. A 409 (1998) 1.
[13] E. Cerron Zeballos et al., Pure avalanche mode operation of a 2 mm gap Resistive Plate Chamber, CERN/LAA-MC, 97-01.